IRAQI BULLETIN OF GEOLOGY AND MINING (IBGM)\
IRAQ GEOLOGICAL SURVEY (GEOSURV-IRAQ)

*IBGM (**2025**, Vol 21; Issue 1)* *257-274*

A CONTRIBUTION TO HYDROCARBONS EXPLORATION: INTEGRATION OF THE GRAVITY METHOD TO REDUCE SEISMIC UNCERTAINTY IN THE SOUTHERN DESERT KARST REGION, IRAQ

Hayder A. Al-Bahadily[1*] and Ali M. Al-Rahim[2]

[1] Department of Geology, Geophysics Division, Iraq Geological Survey (GEOSURV), Baghdad, Iraq;
[2] Department of Geology, College of Science, University of Baghdad, Baghdad, Iraq;
e-mail: ali.m@sc.uobagdad.edu.iq
* *Corresponding author e-mail: hayder.adnan@geosurviraqi.industry.gov.iq*

Type of the Paper (Article)
Received: 28/12/2024
Accepted: 18/02/2025
Available online: 27/ 06/ 2025

Abstract

The study area is the Southern Desert (SD) of Iraq, known for its intensive karst features that are notoriously difficult to image subsurface using reflection seismic survey. Determining the subsurface karst terranes is of extreme importance in the exploration program and mitigation of the associated hazards. This contribution presents the gravity method as an auxiliary method with seismic reflection in detecting subsurface karst forms and determining their precise locations. Appropriate processing and interpretation of gravity data may be extremely helpful in resolving this issue and reducing seismic uncertainty, which is the principal goal of this work. The gravity field of the SD is decomposed into local and regional fields utilizing an upward continuation filter. The residual gravity maps are presented that might be used as an integrated tool in seismic data processing and interpretation, and in mitigating the hazards of the upcoming seismic survey. The near-surface negative anomalies in the SD are mostly linked with karst forms and near-surface density deficiencies. The decomposition is followed by estimating depths to the tops of geological structures using 1D radially averaged power spectrum analyses. A strong relationship between pre-existing exploration wells and positive residual gravity anomalies is found in the study area, indicating that these wells were drilled on structural highs of hydrocarbon interest. The available information on the total drilling depths for three wells shows encouraging results with the estimated depths utilizing the 1D radially averaged power spectrum method. Further, the results show that some wells have been drilled off the crest of the structures of interest. Therefore, this study provides a geophysical means of reconsidering the existing borehole results over relatively shallow structures.

Keywords: karst; geological structures; gravity field separation; seismic reflection problems; Iraq Southern Desert.

ISSN 1811-4539, EISSN 3005-3714
https://doi.org/10.59150/ibgm2101a15
IBGM: http://ibgm-iq.org/
Academic Scientific Journals: www.iasj.net

1. Introduction

The Southern Desert (SD) of Iraq (Figure 1) is characterized by intensive karstification, creating a complex and challenging geologic environment e.g., (Xeidakis, G. S. et al., 2004) (V. Sissakian et al., 2015). This environment complicates subsurface imaging obtained by the seismic reflection method (Chalikakis et al., 2011; Grandjean & Leparoux, 2004). Dissolution structures in the karst geology cause severe attenuation in acoustic impedance energy e.g. Park et al. (1998), resulting in poor seismic quality, noncontinuous reflectors (Mohammed, 2006), and limited imaging depth (Leonard, 2000 in Grandjean & Leparoux, 2004). In such conditions, integration with another geophysical method, mainly the potential methods (gravity and magnetic), is essential (S. I. Shevchenko & Iasky, 2004); Ai et al., 2024a; AI et al., 2024b; (S. Shevchenko, 2017); Filina et al., 2019; Filina et al., 2020) for increasing the resolution and definition of geologic structures underlying karstified zones. The study area includes the karst terrain delineated by Hamza (1997) and spans approximately 180 Km × 130 Km. Many geophysical and geological studies (e.g., Al-Bahadily et al., 2024a; Sissakian et al., 2015) show that the karst region is larger than that previously delineated by Hamza (1997). Therefore, this study deals with the whole SD as a karst-affected area within the Iraqi territory.

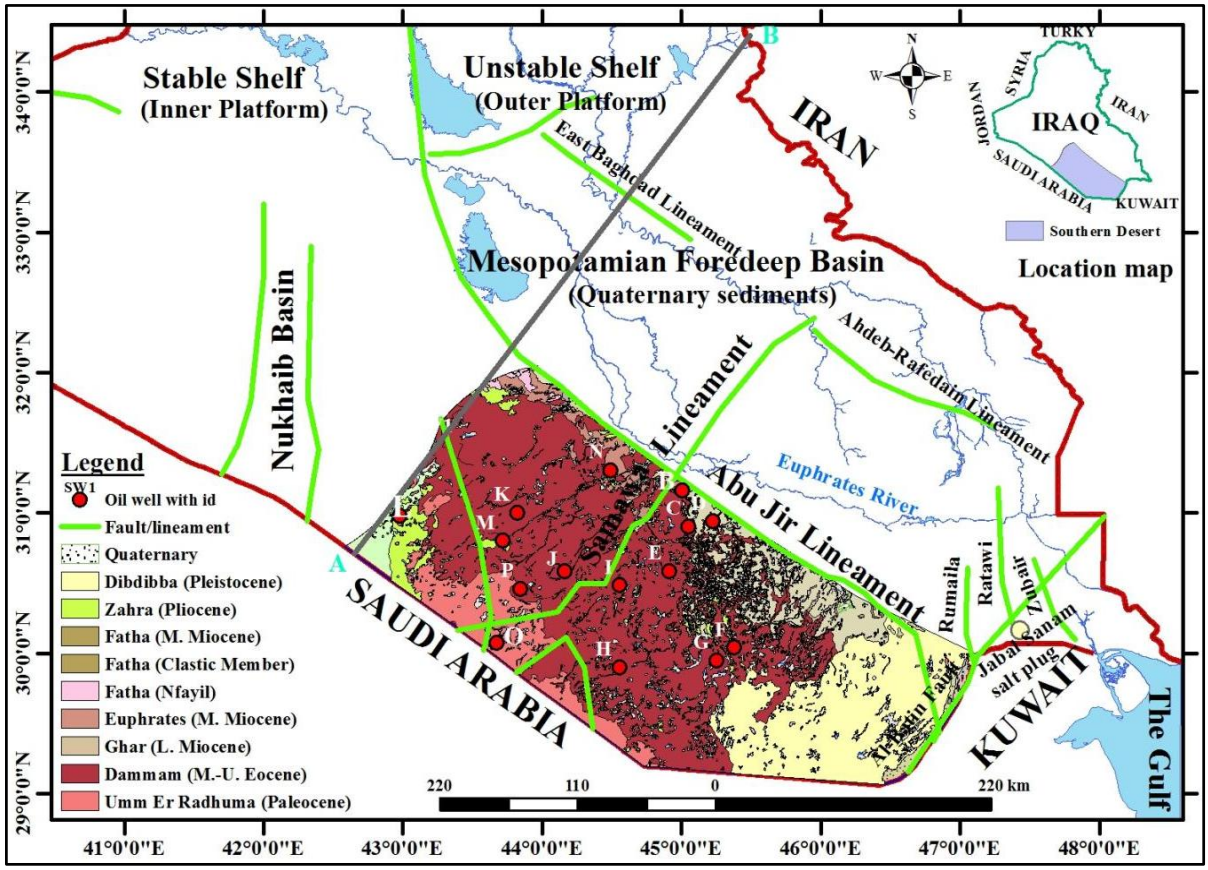

Figure 1. Geological map of the Southern Desert (V. K. Sissakian & Fouad, 2015) illustrated within the tectonic framework of Iraq (A. A. Aqrawi et al., 2010; Buday, T. and Jassim, 1984; Fouad, 2015), profile AB indicates a megaseismic section shown in Figure 3a.

Removing or minimizing the gravitational effects of karst and other near-surface density inhomogeneity in the SD could also aid the seismic data processing, i.e., velocity analysis and migration stages, and plan for a new seismic survey. The study area is covered by a dense network of seismic reflection surveys, which is considered an essential geophysical method for hydrocarbon exploration (seismic lines network map of Iraq, unpublished, Oil Exploration Company).

The SD is generally described by thick sedimentary sequences, not less than 5.5 Km in its eastern part. The sequences extend in age from Infracambrian, inferred by the Jabal Sanam salt plug, which sits just 40 Km to the extreme eastern corner of the SD (Figure 1), to sediments-filled depressions of Quaternary age. The importance of discovering deep geological structures could be explained by a stratigraphic study published by Aqrawi (1998) for the Paleozoic successions. For the first time, the author considered that the Paleozoic in the SD is a hydrocarbon prospect.

This work has a twofold aim; the first is to define the subsurface density anomalies, including those resulting from the effect of the karst terrane. The second is to enhance the gravity responses of shallow geological structures of interest to hydrocarbon prospectivity and estimate their depths. The karst landscape is dominated by the Dammam Formation and possibly earlier limestone, dolomite, and evaporitic (Rus Formation) formations (Figure 1).

2. Geological Background

The SD lies in the southwestern region of Iraq and covers some 76,000 Km^2 (Figure 1). The SD occupies a position within the Inner Arabian Platform (Fouad, 2015) or the stable part of the Arabian Shelf (Buday, T. and Jassim, 1984). It is bounded from the northeast by the Mesopotamian Foredeep Basin (Unstable Shelf), which is part of the Outer Arabian Platform, along the Abu Jir Fault Zone/Lineament (Figure 1). The Abu Jir Fault Zone is an NW – SE-trending transition zone that varies in width up to 100 Km and extends in depth from the lower crust to the Earth's surface (Al-Banna & Ali, 2018). The main surface characteristic of the study area is a stony plateau landscape that gently slopes northeastward in altitude from around 400 m to 20 m above sea level. The plateaus feature linear valleys, such as Wadi Al-Batin in the extreme southern boundary, and structural cliffs, which are well recognized along the western side of the Abu Jr Fault Zone (Figure 2). Ma'ala (2009a) stated that these plateaus were developed during two tectonic phases. The first phase began after the Oligocene uplift, forming older plateaus that experienced the onset of karstification. The second phase formed the younger plateaus from the Pliocene onward.

The regional strike of the strata is NW – SE with an estimated dip of 2° – 3° towards the NE. The main valleys follow a SW – NE trend, which is perpendicular to the Zagros trend, and are filled with Quaternary sediments (Figures 1 and 2). Many faults of various types, extensions, and displacements are determined on the geologic map of the scale of 1:000,000 (V. K. Sissakian & Fouad, 2015). An overview geological map of the SD is presented in Figure 1.

As is the case in the other regions of Iraq, the deepest exploration well in the study area, well D (see Figure 1 for location), does not reach the basement. It has only penetrated the Late Permian Chia Zairi Formation, with a total depth of 5483 m below sea level (Table 1). Therefore, our information about the postulated basement composition and construction is primarily based on available magnetic data and, to some extent, on gravity data.

3. Karst in the Southern Desert

Karst features are quite common within the Dammam Formation (Middle-Late Eocene) (Figure 1), exhibiting various sizes, shapes, and depths (Figure 2). This suggests different stages of evolution and is frequently bounded by fracture sets. These karst forms are noticeable as scattered typical karst, including the largest karst feature, "Salman Depression". The depression is visible in satellite images (Figure 2, white polygon outlined in red). The thickness of the Dammam Formation increases southeastward from 100 m in the central part of the SD to more than 200 m, as constrained by borehole data (Tamar-Agha & Al-Sagri Kh, 2015).

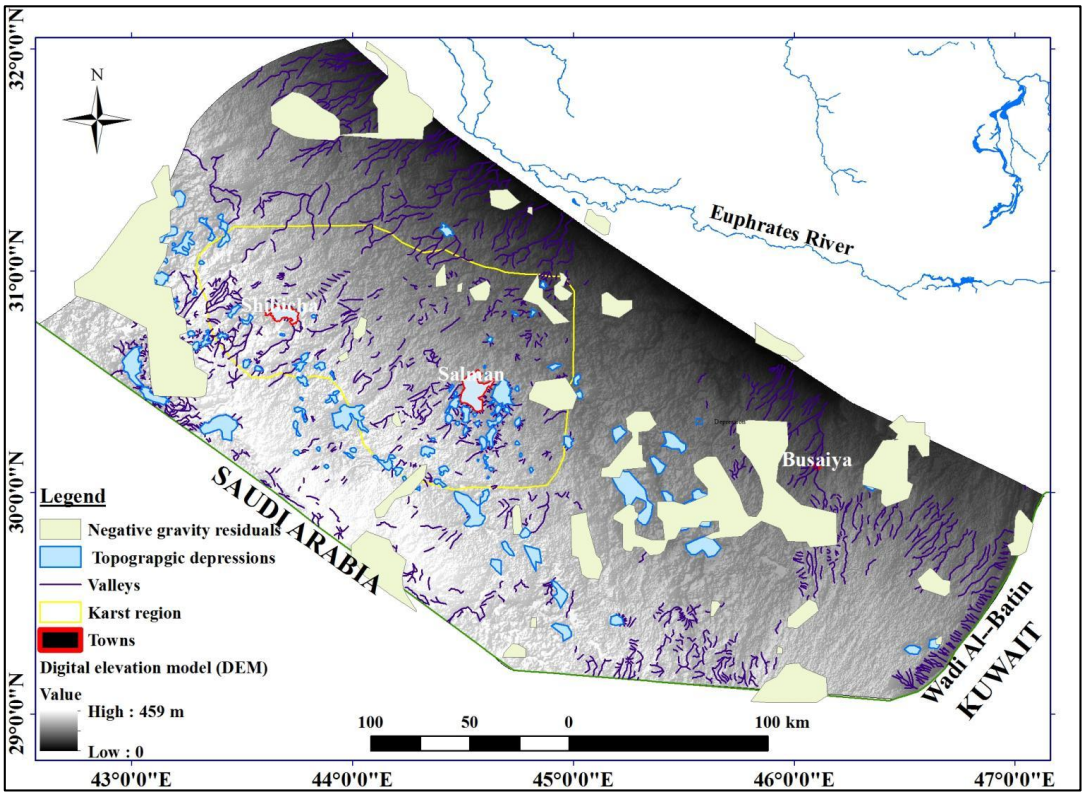

Figure 2. Satellite image of the Southern Desert, including the Salman area, the largest karst Depression. The image has a 12.5 m spatial resolution. The yellow outline represents the karst region delineated by Hamza (1997). Note the topographic depressions (dark blue polygons filled with light blue) some of which are related to karst forms due to the dissolution of carbonate rocks of the Dammam Formation, for example, the largest depressions; the Salman and Shibicha which are outlined by red [the images from ALOS PALSAR (https://asf.alaska.edu/), retrieved in June 2020].

Table 1. Stratigraphy of the Southern Desert inferred from well **D**. The total depth is 5483 m (below sea level).

PERIOD	EPOCH	FORM-ATION	DEPTH (m)	LITHO-LOGY	DESCRIPTION
TERTIARY	EOCENE-PALEOCENE	Dammam	122		Limestone interbeded with anhydrite and dolomite
		RUS	202		Anhydrite interbeded with dolomite
		Umm-Er Radhuma	646		Dolomite and Anhydrite
CRETACEOUS	UPPER	Tayarat	754.5		Dolomite and Shale
		Shiranish	934.5		Limestone with Silt and Shale
		Hartha	1032.5		Limestone with Marl
		Safawi	1276		Dolomite with Anhydrite
		Sadi	1411.5		Chalky Limestone interbeded with Dolomite
		Tanuma	1467.5		Shale with Marl and Limestone
		Khasib	1496.5		Limestone with Shale and Marl
		Kifil/Mishrif	1533		Limestome Silty anhydrite, Marl with Anhydrite & Shale
		Rumaila	1597.5		Limestone and Dolomite
		Ahmadi	1734.5		Marl with Shale and Limestone
	Lower	Mauddud	1759.5		Compacted Limestone
		Nahr Umr	1950		Friable Sandstone with Limestone
		Shuaiba	1985.5		Dolomite, silty
		Zubair	2534		Altrnative Sandstone with Siltstone
		Ratawi	2629.5		Dolomite interculated with Sandstone and Limestone
		Yamama	2730		Limestone with Shale
JURASSIC	Upper	Sulaiy	2761		Silty Limestone
		Gotnia	2815		Chalky Limestone
		Najmah	3236		Limestone chalky with Silty Limestone with Anhydrite
	Middle	Sargelu	3603		Shale and clyey Limestone, Chalky Limestone
	Lower	Alan	3679		Chalky Limestone with Anhydrite
		Mus	3770		Limestone with Dolomite and Shale
		Adaiyah	3875		Limestone with Dolomite and Anhydrite
		Butmah	4169		Dolomite with Shale, marl and Anhydrite
TRIASIC	Upper	Kurra Chine	4575		Anhydrite with Limestone, dolomite and all of salt with Shale
	Middle	Geli Khana	5085		Dolomite with Limestone , Anhydrite with Shale
	Lower	Beduh	5111		Shale and Anhydrite
		Mirga Mir	5210		Limestone with Anhydrite and Shale
PERMIAN		Chia Zairi	5483		Silty Limestone with Shale and Anhydrite

The Salman Depression, located in the central region of the SD, is 20 Km long with variable widths and depths ranging between 4.5 – 10 Km and 5 – 35 m, respectively. It is comprised of three merged depressions (V. K. Sissakian et al., 2013). The available data on the thickness of the Dammam Formation suggests the average thickness of the karst zone is about 150 m. The large volume of dissolved rocks in the Salman and Shibicha depressions (Figure 2), as well as other karst terrains and forms filled with Quaternary sediments, should be investigated. It reflects the complexity and volume of the subsurface drainage system that developed during the evolution of the regional karst system.

Therefore, the involvement of earlier deposits of shallow water limestone, dolomite, and evaporitic formations, Rus (Early Eocene) and Umm Er Radhuma (Late Paleocene) Formations in the karst process are not excluded (the surface extensions shown in Figure 1 can be compared with depth extensions in Table 1). In karst systems, large-scale and connected subterranean karst forms, like the three connected surficial karst forms of Salman, Shibicha (Al-Sa'ah), and other scattered and unnamed depressions, are often expected. For large-scale karst forms such as these, it is speculated that the national gravity data can help define the subsurface density contrast resulting from these features. Al-Bahadily et al. (2024a) suggest a local mantle doming underneath several of the larger karst collapse structures. Additionally, they mentioned that the doming and associated mantle uplift, tectonically connected with the onset of the Mesopotamian Foredeep Basin (~18 Ma; Saura et al., 2015). The doming, which underlies the local karst subsidence, is suggested to be tectonically related to fracture enhancement in the later succession of carbonate formations, leading to large-scale karst depressions.

4. Data, Methods, and Software

Understanding the karst terrane helps comprehend the underlying geological structural relationship to the karst terrain, primarily using national gravity data. The data have been reprocessed and formatted into a Geosoft database as fully terrain-corrected complete Bouguer products by GEOSURV and GETECH (GEOSURV and GETECH Group plc., 2011; Lei et al., 2011). The total station count is 121119. The Location of fifteen hydrocarbon exploration wells lying within the study area (Figure 1) is used in this study to show their positions relative to the residual gravity anomalies. Further, these locations are compared with interpreted geological structures that will be obtained from the results of this study. The available information on the depths of geological structures of hydrocarbon importance ranges between 1585 m and 5483 m (below sea level). This range includes the Mesozoic and the upper part of the Paleozoic (Table 1).

The upward continuation technique is used to separate the gravity field, while the power spectrum analysis is used for in-depth estimation. Considering the scale of the present gravity survey relative to the size of subsurface karst forms to be detected, small-scale karst forms cannot be detected at such a relatively regional scale. The estimated depths are then compared with the depths of the available exploration wells to validate the results of the method used.

The logarithmic power spectrum analyses and depth estimates are performed utilizing GETgrid software, Resolve v1.255 (Plc, 2003).

5. Megaseismic Line

The interpreted seismic section (Line 7) was constructed by Mohammed (2006) across Iraq utilizing 16 pre-existing seismic reflection lines that were measured between 1975 and 1983. This line extends about 500 Km, beginning from the Iraqi-Saudi border in the southwest, passing through the Al-Ma'aniyah Depression at the extreme northwest of the study area, and reaching the Iraqi–Iranian border in the northeast. The section (Figure 3a) and the line, as drawn on the tectonic map of Iraq (Figure 1), are used to highlight the poor quality of the seismic section (Figure 3b). In addition, we can compare the quality of the SD with that part of the Mesopotamian Foredeep Basin.

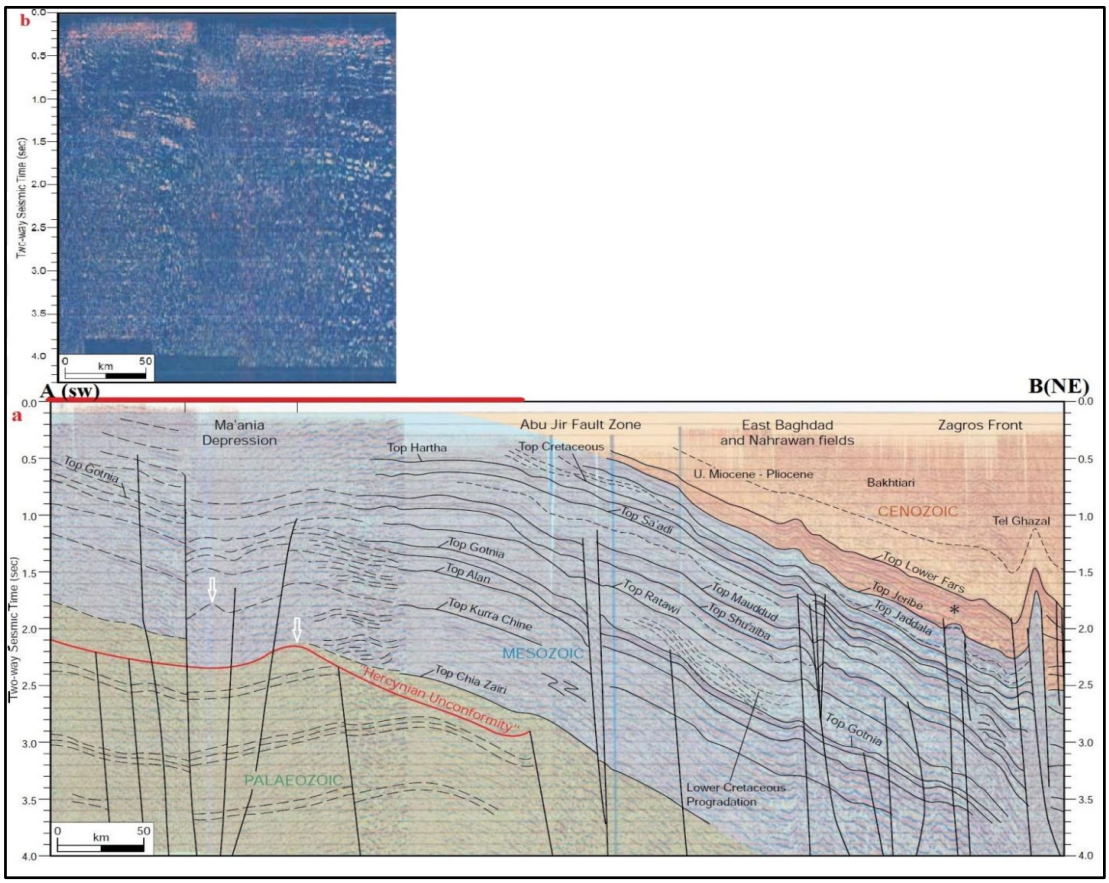

Figure 3. a) Interpreted megaseismic line (AB) passing across the northern boundary of the Southern Desert (SD) through NS trending Al-Ma'aniyah (written Ma'ania) Depression, NW – SE trending Abu Jir Fault Zone, and the Mesopotamian Basin, for the location of the line, see Figure 1. Note the faulting and uncertain seismic horizons over Al-Ma'aniyah compared with continuous horizons in the Mesopotamian Basin. The thick red line in the upper left margin outlines the approximate extent of the SD. White arrows are examples of anomalous structures/ features. b) Original seismic sections start from "A" of the megaseismic line {AB, shown in (a)} within the SD, indicating the bad quality reflections (modified from Mohammed, 2006).

Figure 3a displays an interpreted megaseismic line (AB) that traverses the northern boundary of the SD, passing through the NS-trending Al-Ma'aniyah Depression, the NW–SE trending Abu Jir Fault Zone, and the Mesopotamian Foredeep Basin. The section clearly shows the poor data quality over the study area, resulting from near-surface heterogeneity, including the karst effect (Figure 3b). This uncertainty in the seismic image necessitates integrated geophysical imaging to reveal the geological structures of interest. It is worth noting that these structures were developed due to faults affecting both the basement and sedimentary cover (Figure 3a). They most likely formed to accommodate the tectonic stresses resulting from the convergence of the Arabian and Iranian (portion of Eurasian) Plates. The convergence has been continuing since its beginning in the Late Cretaceous (latest Maastrichtian) up to Recent (Ma'ala, 2009b). The available information suggests that some of these structures have not yet been discovered, as is also shown in a recent study carried out by Al-Bahadily et al. (2024a).

6. Gravity Data and Depth Estimates

The Iraq Petroleum Company (IPC) and the Iraq Geological Survey (GEOSURV) jointly acquired the national gravity survey, providing coverage across the entire Iraq territory except for the highly folded zone. The gravity survey of the SD was initially surveyed for the IPC in 1945. Later, in the 1980s, this survey was seamlessly compiled with the other regions of Iraq to produce the unified Bouguer gravity map of Iraq (Abbas et al., 1984).

The SD is covered by NS- and EW-oriented profiles with line spacing varying from 4.0 to 5.5 Km and a station spacing (in-line spacing) ranging between 0.5 Km and approximately 1.0 Km. The fieldwork was conducted by Robert Ray Co. using the loop technique, achieving an accuracy of ~0.05 mGal. The gravity map of the SD, presented in Figure 4, is the Decompensative Anomaly (DA) map, which represents the gravity effects of the upper crust (Cordell et al., 1991).

The power spectrum analysis plot typically exhibits three segments, which can be fitted by straight lines of different slopes decreasing with increasing wavenumber (Spector & Grant, 1970). These slopes typically represent deep sources, intermediate sources, and noise corresponding to high-, intermediate-, and low-wavenumber, respectively. In this study, only the middle slope is utilized to estimate the depth to the top of the geological structure of interest.

One notable advantage of using this depth estimation approach is that the rate of energy decay of gravity sources remains constant regardless of the upward continuation height used. This means that we obtain the same depth estimations even when several upward continuation levels are applied to the data, without needing to correct the elevation level of data resulting from the second upward continuation level (Jacobsen, 1987).

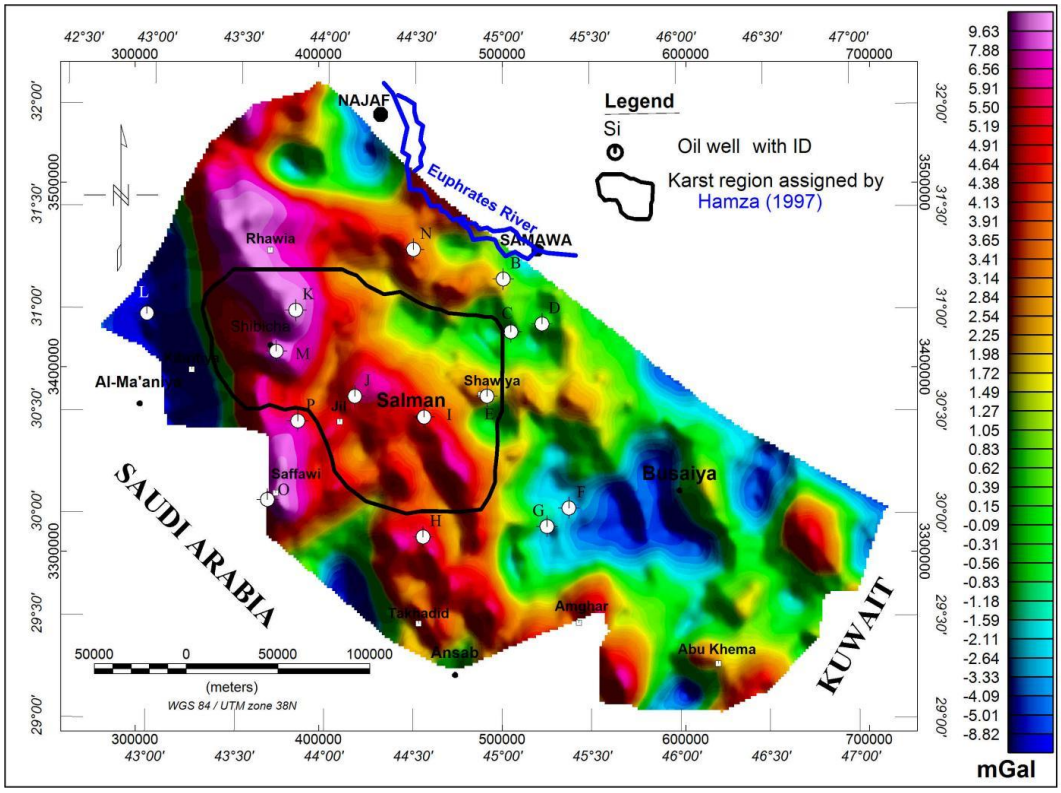

Figure 4. Gravity map of the Iraqi Southern Desert. The map is utilized in gravity data processing and interpretation.

7. Results

7.1. Regional-Residual Separation of the Gravity Field

The DA field of the SD (Figure 4) is separated into regional and residual components utilizing the upward continuation filter and applying the technique of (Jacobsen, 1987). Two residual maps are obtained; the first represents the gravity responses of the near-surface density inhomogeneity, demonstrated in Figure 5. It implicates the effects of the karst region, including those delineated by Hamza (1997), and the effect of noise. However, the effect of noise includes all residual gravity amplitudes that have values ≤ 0.05 mGal. The residual anomalies in Figure 5 are highlighted as negative (blue) and positive (red) anomalies. This map is obtained by subtracting a regional field calculated by applying a 500 m upward continuation filter (see Figure 6a) to the DA field (Figure 4). In Figure 5, the negative anomalies, which have amplitudes ≥ -0.05 mGal, are related to subsurface density deficiencies and the possible karst terrane in the SD. Approximately, the amplitude values of the residual anomalies lie between -0.40 and + 0.35 mGal. In Figure 5, we have applied a threshold value of -0.1 mGal, which is twice the accuracy, to display only reliable negative anomalies, which may be subsurface karst forms (terranes). The results are posted as yellow polygons on the satellite image of the SD for comparison with the surface depressions (Figure 2).

A second residual map is calculated using the same technique but utilizing a different regional field. This map defines the subsurface geological structures, whose gravity responses could be obscured by the impact of near-surface density inhomogeneity (Figure 5) overlying them. To obtain this residual map, a 5000 m upward continuation filter is applied to the DA grid. The resulting grid represents a second regional field that is subtracted from the DA field (Figure 4), resulting in the map in Figure 5.

Then, the effect of the near-surface residual map (the residual grid of the 500 m upward continuation; Figure 5) is subtracted from the residual of the 5000 m upward continuation. This produces a second residual map displayed in Figure 7. The 5000 m upward continued DA field is shown in Figure 6b, exhibiting the gravity responses of deeper sources, and the field appears much smoother than in Figure 6a.

The map depicted in Figure 7 illustrates the gravity responses of relatively shallow geological structures and is devoid of the gravity responses of the karst zone and other near-surface density inhomogeneities. In Figure 7, the positive and negative residuals at longer wavelengths assumed deeper levels, are enhanced. These residuals are more readily available for further qualitative and quantitative interpretations, including depth estimates.

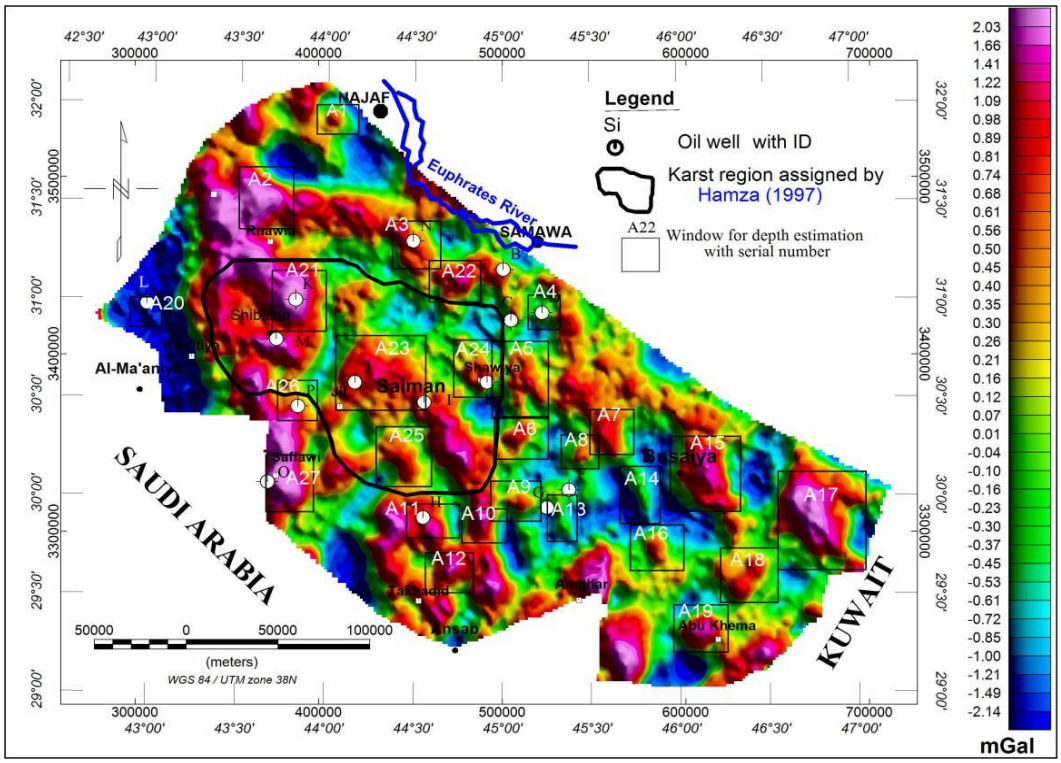

Figure 5. Residual gravity map showing the gravity responses of the near-surface density inhomogeneity, including the karst terranes/ terrains of the Southern Desert. Black-color polygon outlines the karst region delineated by Hamza (1997).

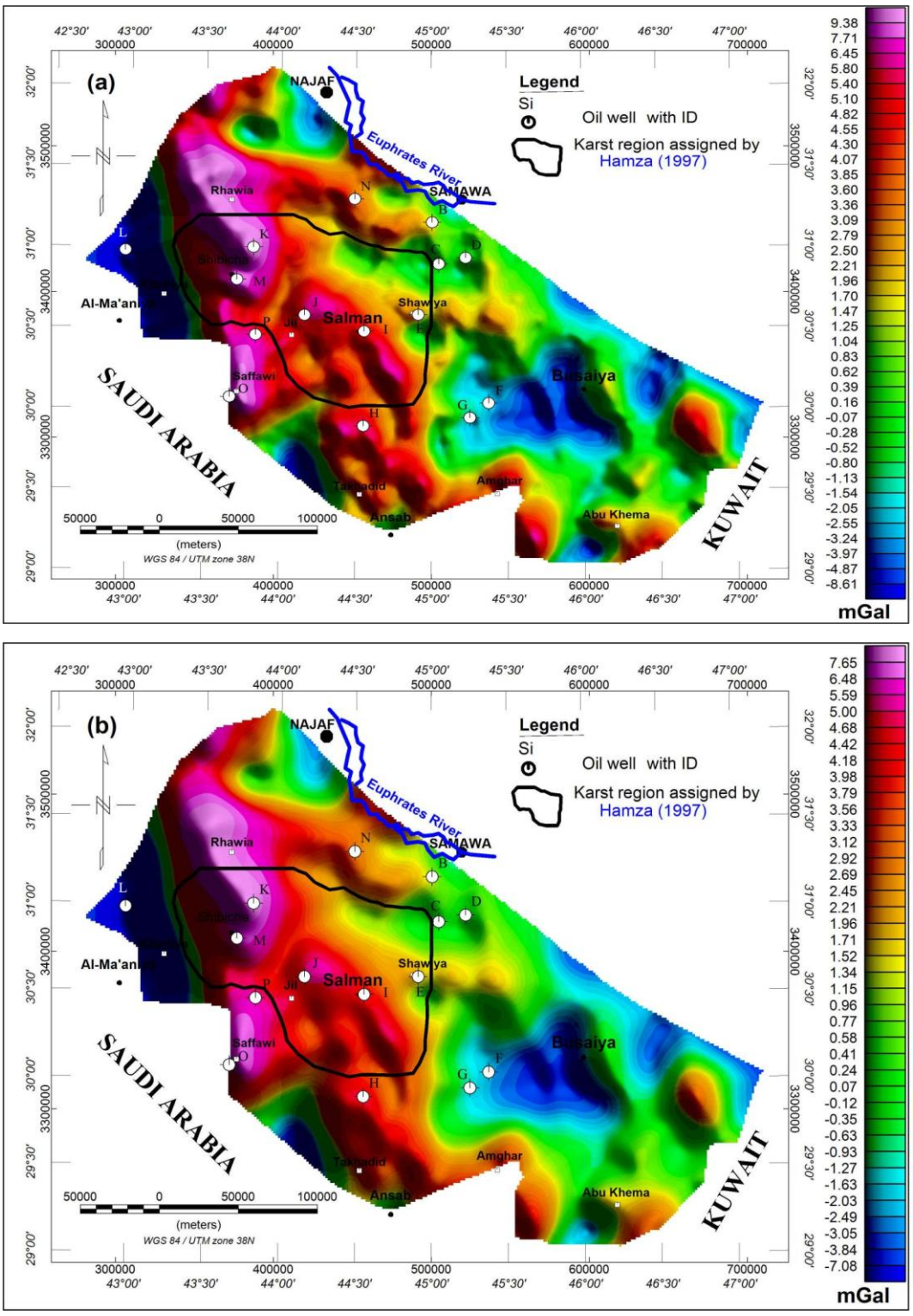

Figure 6. The regional gravity field of the SD was calculated by the upward continuation filter at a height level of (a) 500 m and (b) 5000 m. Anomalies in (b) appear much smoother than in (a) due to the effect of increasing distance between the measuring surface and gravity sources (or upward continuation) on the gravity field.

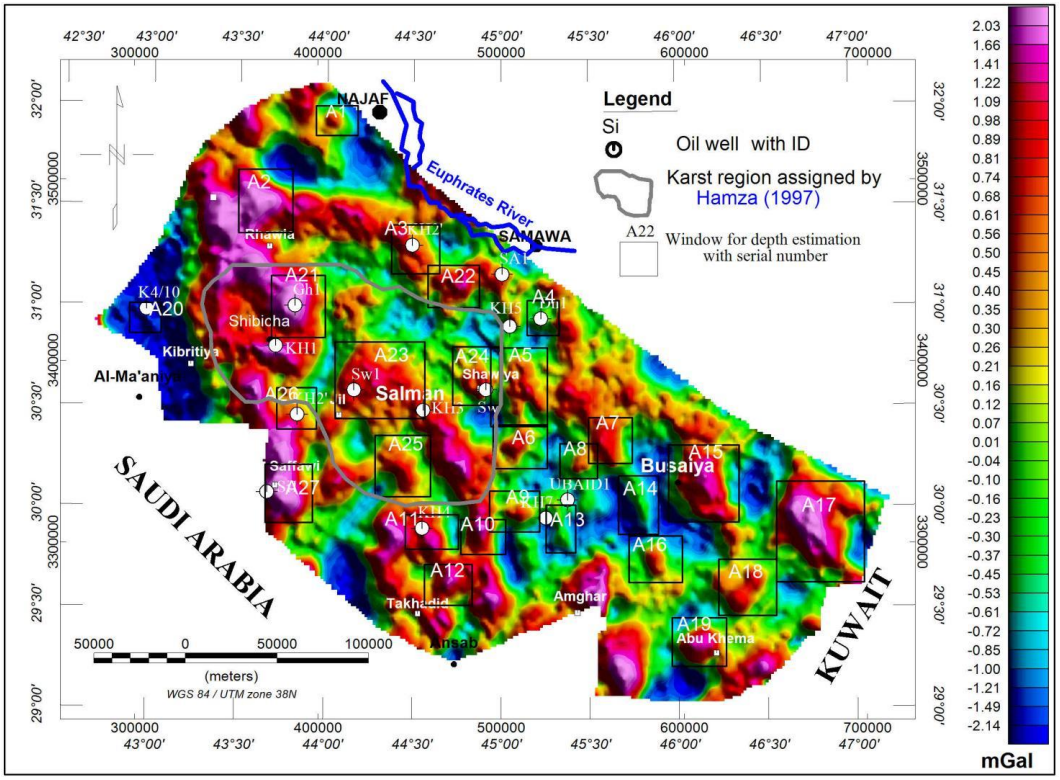

Figure 7. Residual gravity map of the Southern Desert obtained from a 5000 m upward continuation filter and devoid of near-surface gravity effects, including the karst terranes. The map highlights the positive gravity residuals that most likely are important in hydrocarbon exploration since they could be geological structures. The black boxes represent windows used in 1D-power spectrum analyses for depth estimation, with a number inside indicating an anomaly number. For a description, refer to the text.

7.2. Estimation of Depths to the Tops of Geological Structures

After enhancing the gravity anomalies, which could be related to relatively shallow geological structures, these anomalies become more readily available for quantitative interpretation. Some positive gravity residuals, outlined by black-color boxes in Figure 7, are selected for 1D radially averaged power spectrum analysis for depth estimations to the tops of geological structures.

Twenty-seven positive residual anomalies of different sizes and amplitudes, surrounded by black boxes with their anomaly numbers (ID) from A1 to A27 (Figure 7), are chosen for depth estimates. Utilizing the GETgrid software, the average depth to the tops of the gravity source (geologic structure) is estimated using the method proposed by Spector & Grant (1970), as mentioned in Section 6. The estimated depths, in meters, range between 1120 m and 6980 m, as presented in Table 2. Figure 8 illustrates an example of the depth estimate for anomaly no. 26 (A26), which has an estimated depth of 2900 m (see Figure 7 for location).

The total depths of the available exploration boreholes are displayed in bold black color in Table 2 alongside the corresponding estimated depths obtained from 1D radially averaged

power spectrum analyses. The calculated depths, as shown in Table 2, mostly represent the depths to the tops of geological structures within the Mesozoic Period. However, the relatively high depth values could indicate structures or features within the Paleozoic Period (Figure 3a), white arrows at the dashed-black (Kurra Chine Formation), and red surfaces (Hercynian Unconformity, respectively).

Table 2. Depth to the top of geological structures estimated from 1D radially averaged power spectrum. Bold numbers indicate the true depth obtained by drilling.

ID	Estimated Depth in meters below sea level	ID	Estimated Depth in meters below sea level
A1	2630	A15	3230
A2	5070	A16	4630
A3	3530	A17	4150
A4	4930, **5483 (D)**	A18	5250
A5	3230	A19	4060
A6	3700	A20	1650
A7	6980	A21	1120
A8	6790	A22	1800, **2340 west of (B)**
A9	3230	A23	1750, **1730 (J)**
A10	5750	A24	1850
A11	6610	A25	2300
A12	4330	A26	2900
A13	3440	A27	5180

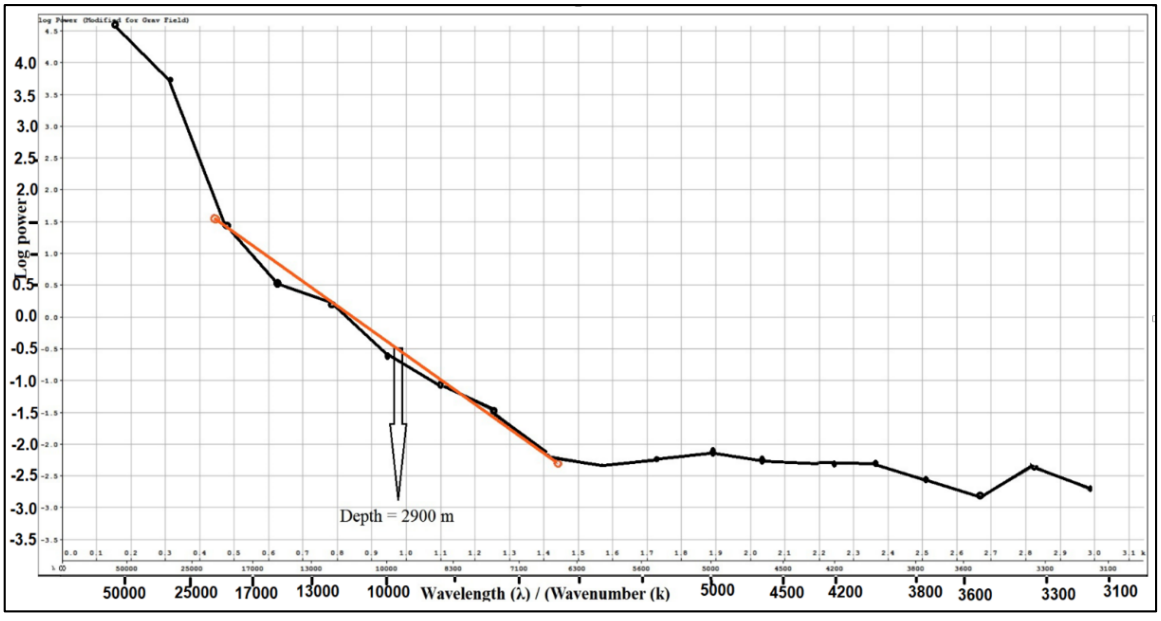

Figure 8. Logarithmic radial power spectrum plot for gravity anomaly no. 26 (for location, refer to Figure 7) shows the estimated depth from the middle slope; blue line. For a description, see the text.

8. Discussion

The quality of the gravity data is suitable for a regional survey, principally conducted for oil exploration purposes. Therefore, small-scale karst forms are not anticipated to be covered in this survey, and anomalies of low amplitudes cannot be dependable when they are equal to or less than the accuracy of measurement (±0.05 mGal). In Figure 5, we noticed that the positive residuals dominate, with amplitude ranges from 0.05 to 0.31 mGal. The positive residuals represent regions that are less or not affected by karst processes. Conversely, the negative residuals, which are considered to be possible karst structures, align in the NS and NW – SE directions, similar to surface depressions (Figure 2). These directions were reported by Sharland et al. (2001) and Jassim et al. (2006) as basement-inherited weak zones, suggesting reactivation of these zones.

The map shown in Figure 5 can identify karst terranes and other near-surface inhomogeneities only when they are of a regional scale and compatible with the nature of gravity survey parameters. The negative anomalies are distributed throughout the study area in different amplitudes and dimensions. This map was not previously available. The negative anomalies should be considered in future seismic surveys and drilling programs, as they potentially reflect the responses of the karst terrane. Therefore, it would be beneficial to conduct a detailed gravity survey of 100 m spacing intervals to investigate a few "important" negative residuals. These residuals are characterized by high amplitudes, wide extensions, and no surface expressions. Positive anomalies could reflect the hardness of subsurface rocks relative to their surroundings, and thus, they may indicate optimal tracks for upcoming seismic surveys.

In Figure 5, gravity effects from deep-seated sources still appear, indicating a rather incomplete separation. For instance, the wide NS-trending negative anomaly in the extreme northwest Al-Ma’aniyah depression has been confirmed in many geophysical studies e.g. Al-Bahadily et al. (2024), Al-Bahadily et al. (2024b), and Al-Bahadily et al. (2024c) as a basement-related graben. The incomplete separation is expected in such a complex geological environment because there is a common overlap in the wavelength contents between deep and shallow sources. As a result, optimal separation in the frequency domain is difficult, if not impossible.

The map of gravity highs presented in this study (Figure 7) was also not previously available. This map is important because it provides an image of direct targets (structures) for seismic reflection survey after removing/ minimizing the near-surface density inhomogeneity, including karst effects. In addition, depths to the tops of the interpreted geological structures are made available from gravity data jointly with depth maps acquired by seismic inversion and borehole information. The certainty of the calculated depth using 1D radially averaged

power spectrum analysis depends mainly on data quality and the structural complexity of the area. An isolated source offers a clear analysis, which facilitates dividing the plot into three separate segments and helps estimate the average depth from the intermediate one.

Other integrated studies are suggested to further improve this work. For instance, the apparent density model of near-surface inhomogeneity helps estimate velocity and its vertical and lateral variations. In addition, the qualitative interpretation of magnetic maps could assist in determining basement fault systems. These may coincide with the lineament analysis technique suggested by Holden et al. (2011), which is useful in seismic data processing and interpretation. Basement-reactivated faults enhance/evolve faults and fractures in the upper sedimentary strata that significantly affect seismic energy. These basement faults can be inferred from studying magnetic data (Al-Bahadily et al., 2023); (Al-Bahadily et al., 2024b) and (Al-Bahadily et al., 2024c).

The maps, shown in Figures 5 and 7, might be utilized as an integrated tool for seismic data processing and interpretation in the SD. Additionally, the interpretation adopted in the present study provides a basis for the planning of drilling programs. This determines the appropriate location for drilling boreholes at structural highs. A strong relationship between the exploration wells and positive residual gravity anomalies, shown in Figure 7, is evident in the study area. This encourages discovering other similar anomalies not yet drilled and suggesting them as structural highs of hydrocarbon interest. The available information on the total depth of three wells, D, B, and J, shows reliable results of estimated depths to the tops of the geological structures using the 1D radially averaged power spectrum method. Furthermore, the results show that the previously drilled wells (E, O, M, N, and K), based on seismic survey results, were drilled off the crest of these structures of interest. This reveals the importance of using the gravity method as an excellent interpretation tool to assist seismic surveys in karst-dominated areas.

9. Conclusions

The method used in the research can be applied to areas that suffer from caustic problems as a result of being affected by karst formations within the stable parts of the platforms. The present work addresses the problem associated with seismic surveys in areas characterized by intensive karst phenomena. Gravity data are integrated with seismic reflection data in the Southern Desert of Iraq. Gravity data could be used to interpret seismic reflection, especially in areas characterized by difficult subsurface imaging. Some examples of such areas are karst-dominated areas and high near-surface density heterogeneity, in which using gravity findings could minimize seismic uncertainty. After separating the gravity field, two residual maps are presented (Figures 5 and 7). The first map reveals near-surface anomalies related to density inhomogeneity and karst terranes. The considerable negative anomalies and surface

depressions exhibit a noticeable NS and NW-SE alignment, compatible with two basement-inherited fault zones, suggesting the reactivation of these zones. These anomalies are valuable for understanding subsurface issues that commonly affect seismic surveys. The second map displays gravity highs, which could be interpreted as structural highs of interest in hydrocarbon exploration. Depths to the tops of these structures are estimated using 1D radially averaged power spectrum analyses. The accuracy is acceptable, providing supplementary information for seismic interpretation.

Acknowledgments

The authors are highly appreciative of the Iraq Geological Survey (GEOSURV) for providing and acquiring the necessary data, documents, and software. We are grateful to Mr. Andrew J. Long (Subterranes Ltd., UK) for his valuable suggestions, cooperation, and comments, whereby the work as a whole particularly the manuscript was improved drastically. We also thank Mr. Jameel R. Kammona (Geophysicist, Expert at Oil Exploration Company, OEC), for his assistance and support of this work.

References

Abbas, M. J., Al-Kadhimi, J., & Fattah, A. S. (1984). Unified Gravity Map of Iraq. In *unpublished int. report, GEOSURV*.

Ai, H., Deniz Toktay, H., Alvandi, A., Pašteka, R., Su, K., & Liu, Q. (2024b). Advancing potential field data analysis: the Modified Horizontal Gradient Amplitude method (MHGA). *Contributions to Geophysics and Geodesy*, *54*(2), 119–143. https://doi.org/https://doi.org/10.31577/congeo.2024.54.2.1

AI, H., EKİNCİ, Y. L., ALVANDI, A., DENİZ TOKTAY, H., BALKAYA, Ç., & ROY, A. (2024a). Detecting edges of geologic sources from gravity or magnetic anomalies through a novel algorithm based on hyperbolic tangent function. *Turkish Journal of Earth Sciences*, *33*(6), 684–701. https://doi.org/https://doi.org/10.55730/1300-0985.1936

Al-Bahadily, H. A., Long, A. J. & Al-Rahim, A. M. (2024a). *Delineation of Karst Features and Underlying Geological Structures in the Iraqi Southern Desert.* Mediterranean Geosciences Union Annual Meeting (MedGU-21), Extended abstract no. 89 (in press)-21).

Al-Bahadily, H. A., Al-Rahim, A. M., & Smith, R. S. (2024a). Determination of reactivated regions and faults in the Iraq Southern Desert with the new edge technique, inverse tilt angle of second-gradients (ITAS). *Acta Geophysica*, *72*(3), 1675–1692. https://doi.org/https://doi.org/10.1007/s11600-023-01176-4

Al-Bahadily, H. A., Al-Rahim, A. M., & Smith, R. S. (2024b). Tectonic elements and structural framework deduced from magnetic data of the Southern Desert, Iraq. *Pure and Applied Geophysics*, *181*(5), 1523–1540. https://doi.org/https://doi.org/10.1007/s00024-024-03460-w

Al-Bahadily, H. A., Fairhead, J. D., & Al-Rahim, A. M. (2024). Structural interpretation of the basement beneath the Southern Desert of Iraq based on aeromagnetic data. *Interpretation*, *12*(3), T209–T219.

Al-Banna, A. S., & Ali, K. K. (2018). The transition tectonic zone between the two parts of the platform in Iraq: A review study. *Iraqi Journal of Science*, *59*(2C), 1086–1092.

Aqrawi, A. A., Goff, J. C., Horbury, A. D., & Sadooni, F. N. (2010). The Petroleum Geology of Iraq. Scientific Press Ltd. *Ed: Beaconsfield UK*, 424.

Aqrawi, A. A. M. (1998). Paleozoic stratigraphy and petroleum systems of the western and southwestern deserts of Iraq. *GeoArabia*, *3*(2), 229–248.

Buday, T. and Jassim, S. Z. (1984). *Tectonic Map of Iraq, Scale 1:1,000,000*. GEOSURV.

Chalikakis, K., Plagnes, V., Guerin, R., Valois, R., & Bosch, F. P. (2011). Contribution of geophysical methods to karst-system exploration: an overview. *Hydrogeology Journal*, *19*(6), 1169–1180. https://doi.org/10.1007/s10040-011-0746-x

Cordell, L., Zorin, Y. A., & Keller, G. R. (1991). The decompensative gravity anomaly and deep structure of the region of the Rio Grande rift. *Journal of Geophysical Research: Solid Earth*, *96*(B4), 6557–6568.

Filina, I., Biegert, E. K., Sander, L., Tschirhart, V., Bundalo, N., & Schiek-Stewart, C. (2019). Integrated imaging: A powerful but undervalued tool. *The Leading Edge*, *38*(9), 720–724. https://doi.org/https://doi.org/10.1190/tle38090720.1

Filina, I., Yalamanchili, R., Re, S., Colombo, D., Price, A., Egorov, V., & Liu, G. (2020). Introduction to special section: Integrated geophysical imaging. In *Interpretation* (Vol. 8, Issue 4, p. SSi-SSv). Society of Exploration Geophysicists and American Association of Petroleum …. https://doi.org/10.1190/INT-2020-0921

Fouad, S. F. A. (2015). Tectonic map of Iraq, scale 1: 1000 000, (3rd edition). *Iraqi Bulletin of Geology and Mining*, *11*(1), 1–7.

GEOSURV and GETECH Group plc. (2011). *Aeromagnetic and gravity data for Iraq; reprocessing, compilation and databasing the aeromagnetic and gravity data of Iraq*.

Grandjean, G., & Leparoux, D. (2004). The potential of seismic methods for detecting cavities and buried objects: experimentation at a test site. *Journal of Applied Geophysics*, *56*(2), 93–106. https://doi.org/https://doi.org/10.1016/j.jappgeo.2004.04.004

Hamza, N. M. (1997). *GEOMORPHOLOGICAL MAP OF IRAQ*. GEOSURV Publications.

Holden, E.-J., Kovesi, P., Dentith, M., Wong, J., & Fu, S. C. (2011). *CET Porphyry Analysis-Oasis montaj*. Geosoft Inc.

Jacobsen, B. H. (1987). A case for upward continuation as a standard separation filter for potential-field maps. *Geophysics*, *52*, 390–398.

Jassim, S. Z., Goff, J. C., & Goff, C. J. (2006). Geology of Iraq (Chapter Two). In S. Z. J. & J. C. G. Dolin (Ed.), *Dolin, Prague and Moravian Museum, Brno* (1st edition). Dolin, Prague and Moravian Museum, Brno.

Lei, K., Fairhead, J. D., Kerrane, T., & Al-Bassam, K. (2011). Reprocessing of Iraq magnetic and gravity data: *International Workshop on Gravity, Electrical & Magnetic Methods and Their Applications.*

Ma'ala, K. A. (2009a). Geology of Iraqi Southern Desert, Geomorphology. *Iraqi Bull Geol Min. Special Issue*, *2*, 7–33.

Ma'ala, K. A. (2009b). Geology of Iraqi Southern Desert, Tectonic and structural evolution. *Iraqi Bull Geol Min. Special Issue*, *2*, 35–52.

Mohammed, S. A. G. (2006). Megaseismic section across the northeastern slope of the Arabian Plate, Iraq. *GeoArabia*, *11*(4), 77–90.

Park, C. B., Miller, R. D., & Xia, J. (1998). Ground roll as a tool to image near-surface anomaly. In *SEG Technical Program Expanded Abstracts 1998* (pp. 874–877). Society of Exploration Geophysicists.

Plc, G. G. (2003). *GETgrid Processing Software Resolve v1.255*.

Saura, E., Garcia-Castellanos, D., Casciello, E., Parravano, V., Urruela, A., & Vergés, J. (2015). Modeling the flexural evolution of the Amiran and Mesopotamian foreland basins of NW Zagros (Iran-Iraq). *Tectonics*, *34*(3), 377–395. https://doi.org/doi:10.1002/2014TC003660

Sharland, P., Archer, R., Casey, D., Davies, R., Hall, S. H., Heward, A., Horbury, A., & Simmons, M. (2001). Arabian Plate Sequence Stratigraphy. In *GeoArabia Special Publication* (Vol. 2).

Shevchenko, S. (2017). The interpretation and integration of old seismic with new gravity data—an example from the northern Perth Basin. *Petroleum Exploration Society of Australia (PESA) News*, *146*, 42–47.

Shevchenko, S. I., & Iasky, R. P. (2004). Is there room for gravity in petroleum exploration or is the door shut? *Exploration Geophysics*, *35*(2), 124–130. https://doi.org/10.1071/EG04124

Sissakian, V., Al-Ansari, N., & Knutsson, S. (2015). Karst Forms in Iraq. *Journal of Earth Sciences and Geotechnical Engineering*, *5*(4), 1–26.

Sissakian, V. K., & Fouad, S. F. (2015). Geological map of Iraq, scale 1: 1000000 (4th Edition). In *Iraq Geological Survey Publications*.

Sissakian, V. K., Mahmoud, A. A., & Awad, A. M. (2013). Genesis and age determination of Al-Salman Depression, south Iraq. *Iraqi Bulletin of Geology and Mining*, *9*(1), 1–16.

Spector, A., & Grant, F. S. (1970). Statistical models for interpreting aeromagnetic data. *Geophysics*, *35*(2), 293–302. https://doi.org/10.1190/1.1440092

Tamar-Agha, M. Y., & Al-Sagri Kh, E. A. (2015). Shading further lights on the Upper Cretaceous–Neogene subsurface lithostratigraphy of the Southwestern Iraq Journal of Science. *Journal of Science*, *56*(1C), 798–827.

Xeidakis, G. S., Torok, A., Skias, S., & Kleb, B. (2004). Engineering geological problems associated with karst terrains: their investigation, monitoring, and mitigation and design of engineering structures on karst terrains. *Bulletin of the Geological Society of Greece*, *36*(4), 1932–1941. https://doi.org/https://doi.org/10.12681/bgsg.16679

About the author

Hayder Adnan Al-Bahadily graduated from the University of Baghdad with a B.Sc. degree in geology/geophysics in 1994, with an M.Sc. and Ph.D. in 1997 and 2022 in geophysics seismic reflection and potential fields interpretation, respectively. Hayder started his career as a field geophysicist with the Iraq Geological Survey in 2000. He conducted several field surveys, including gravity, magnetic, electric, and radiometric. Hayder published many papers in applied geophysics in different fields, including mineral, petroleum, engineering, archaeology, and groundwater. Currently, he is interested in geological (structural and tectonic) data interpretation using geophysical data, especially gravity and magnetic.

e-mail: hayder.adnan@geosurviraqi.industry.gov.iq; hayder.adnan17@gmail.com